JOURNAL OF PROPULSION AND POWER
Vol. 14, No. 5, September–October 1998

Investigation of Heat Transfer and Coking Characteristics of Hydrocarbon Fuels

Keming Liang,* Baoe Yang,† and Zhongli Zhang†
China Aerospace Industry Corporation, Xian, Shanxi 710100, People's Republic of China

In this paper, worldwide investigations of the cooling characteristics of hydrocarbon fuels are reviewed and results of Chinese experimental investigations are presented. The Chinese tests were conducted at pressures of 0.5–30 MPa, flow velocities of 2–106 m/s, and heat fluxes up to 66 MW/m^2. The heat transfer characteristics of methane, propane, no. 21 high-density kerosene, aerokerosene and rocket kerosene in stainless-steel and copper tubes, and the deposit formation rates for kerosene in stainless-steel tubes were investigated. Forced convective heat transfer correlations were obtained for liquid methane, propane, and kerosene. Heat fluxes at which test tubes burnt out were also investigated. The test results indicate that heat transfer coefficients of methane and propane decrease at high wall temperatures, and that the coefficients of kerosene increase at similar conditions because of boiling. No coking was detected in methane tests; coking temperature and coking rates were determined for kerosene in stainless-steel tubes.

Nomenclature

Cp = specific heat
D = diameter
k = thermal conductivity
L = length of heated section
p = pressure
q = heat flux
T, t = temperature
v = velocity
α = heat transfer coefficient
μ = viscosity
ρ = density

Subscripts

b = bulk
cr = critical
in = inlet
s = saturation
w = wall

Introduction

LIQUID oxygen (LOX)/hydrocarbon rocket engines have the advantages of being relatively low cost, low pollution and high performance. The key to the selection of hydrocarbon fuels is their cooling properties. Many kinds of LOX/kerosene rocket engines, such as the H-1, F-1, RD-107, RD-108, etc., were developed and manufactured successfully in the U.S. and the former Soviet Union during the 1950s and 1960s, but the chamber pressures of all these engines were less than 10 MPa. The heat transfer and coking characteristics of hydrocarbon fuels have been investigated since the 1980s.[1–14] LOX/methane and LOX/propane rocket engines have also been demonstrated, but they have not yet been put into practical application. High-pressure and high-performance LOX/hydrocarbon engines currently in practical application are the Russian LOX/kerosene stage-combustion engines, such as the RD-120 and RD-170. In these engines kerosene is successfully used as the coolant.

In China, the heat transfer experiments on the following hydrocarbon fuels were conducted from July 1979 to November 1995: No. 21 high-density kerosene, aerokerosene, propane, methane, and rocket kerosene. The tests were conducted over wide ranges of fluid conditions: Pressures from 0.5 to 30 MPa, flow velocities from 2 to 106 m/s, and bulk temperatures from 288 to 593 K (128 to 143 K for methane), with coolant-side wall temperatures from the ambient to 1070 K, heated section lengths from 30 to 600 mm, inner diameters of the specimen sections from 1.7 to 4 mm, and heat fluxes up to 66 MW/m^2. A detailed summary of all test conditions is presented in Table 1. More than 60,000 test data were obtained in these tests. The heat transfer coefficients of hydrocarbon fuels were evaluated under the preceding test conditions. Forced convection heat transfer correlations were established based on the test data. Coking data and burnout heat flux data were also obtained.

In this paper the cooling characteristics of hydrocarbon fuels and heat transfer test results obtained in China are described and a comprehensive review of this subject is given.

Review of Heat Transfer Investigation of Hydrocarbon Fuels

Heat Transfer Characteristics

Prior to deposit formation, the cooling capabilities of fuels can be completely reflected in the heat transfer coefficients of those fuels. Although different forced convection heat transfer correlations have been obtained for hydrocarbon fuels by various researchers on the basis of their own electrical heat transfer tests, there are two essential forms for all of the correlations. One is in the form of Eq. (1), where the effects of nonuniform property fields caused by the difference between wall temperature and bulk temperature, such as the effects of density, viscosity, thermal conductivity, and specific heat, and the effects of pressure and inlet and outlet conditions are taken into account:

$$Nu = KRe^{a}Pr^{b}(\rho/\rho_{w})^{c}(\mu/\mu_{w})^{d}(k/k_{w})^{e}(\overline{Cp}/Cp)^{f}(P/P_{cr})^{g} \times (1 + 2/L/D)^{m} \qquad (1)$$

The other form is the simpler form of Eq. (2), in which, instead of the property correction terms as in Eq. (1), an absolute temperature ratio $(T_w/T_b)^n$ is used to account for the effect of nonuniform distributions of properties. The subscript w de-

---

Received Sept. 2, 1997; revision received Jan. 25, 1998; accepted for publication March 31, 1998.

*Professor, The 11th Research Institute, P.O. Box 15-11.

†Engineer, The 11th Research Institute, P.O. Box 15-11.

Table 1 Heat transfer test conditions of hydrocarbon fuels

				Heated section			
Propellant	P, MPa	V, m/s	T_b, °C	L, mm	D, mm	Tube material	Number of test data
No. 21 kerosene	12	5–100	20.8–297.8	180	4,2	1Cr18Ni9Ti	4,872
	0.5–30	10	20.8–297.8	180	4	1Cr18Ni9Ti	
	25	10	22.4–267.1	30–600	4	1Cr18Ni9Ti	
	12 (2-h coking test)	10	20.8–297.8	180	4	1Cr18Ni9Ti	
Aerokerosene	12	2–40	11.9–299	180	3	1Cr18Ni9Ti	10,101
	0.5–26	10	11.9–299	180	3	1Cr18Ni9Ti	
	12 (1-h coking test)	10	11.9–299	180	3	1Cr18Ni9Ti	
		20	11.9–299	180	3	1Cr18Ni9Ti	
Propane	12	2–60	10.2–197.9	180	3	1Cr18Ni9Ti	6,384
	2–27.4	10	10.2–197.9	180	3	1Cr18Ni9Ti	
	12 (25-min coking test)	10	10.2–197.9	180	3	1Cr18Ni9Ti	
Methane	5	2–40	−128–130	180	3	1Cr18Ni9Ti	5,925
	0.45–9	10	−128–130	180	3	1Cr18Ni9Ti	
Methane	12	2–106	−124–89	180	3	1Cr18Ni9Ti	3,025
	20	20–40	−124–89	180	3	1Cr18Ni9Ti	
	10–26	10	−124–89	180	3	1Cr18Ni9Ti	
Methane	12	20–90	−145–−77	180	3	Duplex tube with outer steel and inner copper tube	2,025
	1.8–20	40	−145–−77	180	3		
	3.8–20	70	−145–−77	180	3		
Rocket kerosene	0.5–25	10	16–320	100	1.7	1Cr18Ni9Ti, QCr0.5	15,328
	25	10–100	16–320	100	1.7		
	25 (2-h coking test)	10	16–320	100	1.7		
Rocket kerosene	2–15	10	16–320	100	1.7	1Cr18Ni9Ti, QCr0.5	13,280
	15	10–60	16–320	100	1.7		
	15 (2-h coking test)	10	16–320	100	1.7		
	15	60	Inlet temperature 20–200	100	1.7		

Note: 1Cr18Ni9Ti denotes an alloy steel that contains 18% Cr and 9% Ni, and QCr0.5 denotes a copper alloy that contains 0.4–1% Cr.

Table 2 Coefficients and exponents of heat transfer correlation

	Test conditions					Coefficients and exponents										
Fuel	P, MPa	V, m/s	q, Mw/m^2	$T_{b,\text{in}}$, K	T_w, K	k	a	b	c	d	e	f	g	m	n	References
Propane	13.7	6.1–30	——	——	422–811	0.00538	0.8	0.4	−0.125	0.242	0.193	0.395	−0.024	1.0	0	1
RP-1	——	——	——	——	——	0.0056	0.9	0.4	0	0	0	0	0	0	0	2
Methane	——	——	——	——	——	0.023	0.8	0.4	0	0	0	0	0	0	0	
Propane	——	——	——	——	——	0.00696	0.88	0.5	0	0	0	0	0	0	−1.0	
Propane	3.1–12.4	15–45	0.3–16.4	117–394	——	0.00545	0.9	0.4	−1.1	0.23	0.27	0.53	0	1.0	0	3, 4
RP-1 methane	6.9–13.8	30–60	3.1–18.2	230–ambient	230–813	0.044	0.76	0.4	0	0	0	0	0	1.0	0	5
RP-1 propane	6.9–13.8	30–60	3.1–18.2	230–ambient	230–813	0.0068	0.94	0.4	0	0	0	0	0	0	0	6
						0.028	0.8	0.4	0	0	0	0	0	0	0	
Natural gas	6.9–13.8	30–90	3.1–18.2	260–ambient	230–813	3.7	0.42	0.4	0	0	0	0	0	0	0	
Methane	Pin 27–34	55–238	2.6–139	146–275	——	0.022	0.8	0.4	0	0	0	0	0	0	−0.45	7
	——	——	——	——	——	0.023	0.8	0.4	0	0	0	0	0	0	−0.57	14
Methane	——	——	——	——	——	0.023	0.8	0.4	0	0	0	0	0	0	−0.8	14

notes that the fuel properties are evaluated at the wall temperature. All other fuel properties are evaluated at the bulk temperature:

$$Nu = KRe^{a}Pr^{b}(T_w/T_b)^{n} \tag{2}$$

The coefficient and exponent values of the preceding equations in various references are summarized in Table 2.

In the liquid methane tests of Thongchun,[12] a decrease in the methane heat transfer coefficient was detected at supercritical pressures and high heat fluxes. At a pressure of 6.3 MPa, heat flux of 4.4 MW/m^2, and bulk temperatures near the critical temperature of methane, for instance, the wall temperature rose rapidly (from 400 to 900 K) and the heat transfer coefficients decreased significantly (from 1.6×10^4 W/m^2 K to 0.7×10^4 W/m^2 K). This phenomenon also occurred in the liquid methane tests of Giovanetti et al.[5] At a pressure of 14 MPa and heat flux of 11.2 MW/m^2, the heat transfer coefficient was equal to 9.55×10^4 W/m^2 K when the wall temperature was 325 K. The coefficient decreased to 2.44×10^4 W/m^2 K, when the wall temperature was 683 K. To simulate the preceding phenomena at high heat fluxes, the correction factor $(Tw/Tb)^n$ was used for methane and propane. For high supercritical pressure fluids and general combustion gas flow, whose performances are similar to ideal gas, $n = -0.57$, good results could be obtained by using Eq. (2), but it was not suitable for near-critical fluids. Based on the test data on hydrogen and methane at near critical pressure, a bulk expansion factor, ψ_1^+, was obtained by Thongchun[12] to replace the nonuniform property factor T_w/T_b. $\psi_1^+ = 1 + \beta_1^+ \times \Delta T$, where $\Delta T = T_w - T_b$, and β_1^+ is the maximum value of thermal expansion coefficients at temperatures from T_b to T_w. The exponent n should equal -0.30 when ψ_1^+ is used.

The reason for the decreased heat transfer at high heat fluxes has not been clearly explained. The heat transfer rules for low-critical-temperature propellants such as methane and propane may be more complicated than those for kerosene. Valuable test data are provided in our tests, which are presented in the next section.

Coking Characteristics

For hydrocarbon fuels at high temperatures, coking formation and the possible corrosion of cooling channel surfaces can deteriorate fuel-cooling capabilities. Coking of fuels is very dependent on tube material or coatings and on many other factors, such as test duration and intended application (reusable or single-use). The coking temperature limits reported in the following are rough approximations under certain test conditions.

The mechanisms of the corrosion of copper material by hydrocarbon fuels have been studied.[13] The sulfur and oxygen molecules contained in the fuels can sulphurize and oxidize copper, respectively; therefore, the copper wall deteriorates. Another possible cause of copper corrosion is carbon deposition from heated hydrocarbon fuels on a hot copper wall. Compatibility tests conducted by Aerojet[13] for hydrocarbon fuels and copper have shown the following. If the sulfur content is limited to below a certain value, RP-1 can be used until the coolant-side wall temperature reaches 570 K without significant coking and corrosion. If the sulfur content is limited to below a certain value, methane can be used without any coking or corrosion until the coolant-side wall temperature reaches 770 K, but as little as 1 ppm of sulfur in methane can cause the corrosion of a copper wall. When cooling with propane, the sulfur content in the propane must be eliminated completely, and even then, it has not yet been determined whether sulfur-free propane can be used as a coolant for copper walls. These tests indicate the significant effects of sulfur content, especially methyl-hydrosulfide, on channel corrosion. This is in accordance with the Russian kerosene standard, which indicates that the sulfur content in kerosene must be strictly limited and that no methyl-hydrosulfide and hydrogen-sulfide contents are allowed. New comparative analyses of Russian kerosene and RP-1 indicate that the Russian kerosene sulfur content is 21% less than RP-1.[11]

In carbon deposition rates, it has been observed that the deposition rate of methane is lowest in the three fuels.[1,3–5,14] In the tests of Giovanetti et al.,[5] for instance, at a pressure of 13.8 MPa, bulk temperature of 290 K, and velocity of 30 m/s, carbon deposition rates for natural gas in copper tubes did not exceed 0.8 g/m^2 h at wall temperatures between 500 and 650 K. Rates of 2–3.2 g/m^2 h were typical for RP-1 in copper tubes at wall temperatures between 560 and 750 K. The rates for propane in copper tubes were the highest and ranged from 3 to 5.8 g/m^2 h at wall temperatures between 400 and 580 K. Total deposition thermal resistance ranged from 0.001–1 K cm^2/W.

For hydrocarbon fuels, the threshold value of coolant-side wall temperatures is limited by coking considerations. The widely quoted values are 970 K, 700 K (or 730 K), and 560 K (or 590 K) for methane, propane, and kerosene, respectively.[2–4] Considering the coking threshold values, the chamber pressure of the thrust chamber cooled by methane is the highest and that cooled by RP-1 is the lowest. It is known from test data in the published literature that coking occurs at rather low wall temperatures for propane in copper tubes (530 K,[3] 400 K,[5] and 570–610 K[10]) and is more severe than that for kerosene.

Plating the surface of the copper wall with corrosion resistant metals may be a good way to reduce and eliminate fuel coking and channel corrosion. The tests reported by Rosenberg and Gage[14] indicated that gold plating or platinum plating on copper could reduce channel corrosion significantly. Deposition and tube corrosion were also effectively reduced by nickel plating on copper walls.[5] In the Russian LOX/kerosene engine, RD-170, with a chamber pressure of 24.5 MPa, copper is used as the inside wall material with coated silver on the coolant-side wall surface. Combined with other cooling means, the chamber is cooled by kerosene successfully at high pressures and high heat fluxes. In addition, deposition can also be reduced by means of pre-cryogenic cooling of fuels, which is a benefit to thermal stability.

Heat transfer and coking characteristics of hydrocarbon fuels have been studied from different aspects by various researchers. We have investigated the cooling characteristics of the three hydrocarbon fuels over broad ranges of pressure, velocity, and heat flux, and many test data have been obtained at the high temperatures and high heat fluxes that are important for the design of hydrocarbon-fueled engines. These results will be discussed in the next section.

Experimental Results and Discussion

Heat Transfer Experimental System

Two electrical heat transfer test systems were used in our tests: gas pressurized and pump pressurized. A schematic of the gas-pressurized system is shown in Fig. 1. The pump-pressurized system is the same, except that tank I is pressurized by a high-pressure pump. The gas-pressurized system comprises a system for cryogenic tests, such as methane tests, and a system for ambient tests, such as kerosene and propane tests. The volume of the cryogenic tank is 0.1 m^3 with 32-MPa working pressure, and the volume of the ambient tank is 1 m^3 with a pressure of 15 MPa. Nitrogen was used to pressurize the tank in the methane, propane, and rocket kerosene tests and air was used for the no. 21 kerosene tests. Both nitrogen and air-pressurized tests were conducted for aerokerosene. The maximum pressure is 25 MPa in the pump-pressurized system.

The test tubes were made of stainless steel (1Cr18Ni9Ti), and copper (QCr0.5), and duplex tubes were made with an outer stainless-steel tube and an inner copper tube. Five Ni-Cr-Ni-Si thermocouples and five voltage testing points were equally spaced on each test tube for the measurement of tube wall temperature, heating section voltage and total voltage, respectively. The heating current was measured by standard current divider. As shown in Fig. 1, the inlet and outlet bulk temperature and pressure were measured and the flow flux was determined by two turbine flow meters. Two cryogenic flow meters were used in front of the test tube in methane tests. The test tubes were heated by two direct current dynamos with a total power of 288 kW. The dynamos can provide 72 V and 4000 A or 36 V and 8000 A.

Checking tests using drilled water were conducted before all hydrocarbon fuel tests. The energy balance of all the tests is within 10% and most are within 5%. Test data for drilled water correlated well using the following equations:

$$Re < 2 \times 10^4, \qquad Nu = 0.023 Re^{0.8} Pr^{0.4} \tag{3}$$

$$Re > 2 \times 10^4, \qquad Nu = 0.005 Re^{0.95} Pr^{0.4} \tag{4}$$

where the properties are evaluated at bulk temperature. Equations (3) and (4) are the conventional forced-convection heat transfer correlation.

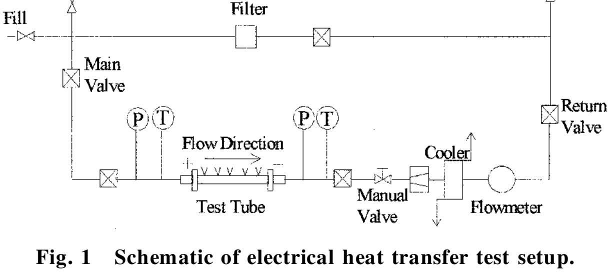

Fig. 1 Schematic of electrical heat transfer test setup.

Kerosene Test

The test conditions for kerosene are given in Table 1, and typical effects of pressure, temperature, and velocity on heat transfer are shown in Figs. 2–4. The effect of pressure on kerosene heat transfer is shown in Fig. 2 for a velocity of 10 m/s and pressures of 0.5–30 MPa. Skin boiling and pseudoboiling for kerosene occurred at subcritical pressures and supercritical pressures, respectively. Pressure had little effect on the heat transfer coefficient before skin boiling or pseudoboiling. Only the boiling temperature was affected by pressure and the boiling temperature increased with increased pressure.

The heat transfer coefficient of kerosene increased with wall temperature increases. The coefficients of kerosene were low at low wall temperatures (shown in Fig. 3), namely, before skin boiling or pseudoboiling and deposit formation, mainly because of the low specific heat and high viscosity of kerosene (Table 3). The heat transfer coefficients increased rapidly after skin boiling or pseudoboiling occurred for kerosene at high wall temperatures. As shown in Fig. 3, for instance, at a pressure of 12 MPa and a velocity of 22.3 m/s, the heat transfer coefficient of kerosene increased from 1.5 × 10^4 W/m^2 K prior to pseudoboiling to 4.8 × 10^4 W/m^2 K after pseudoboiling. The effect of velocity on heat transfer is also shown in Fig. 3. The heat transfer coefficient increased with increases in velocity.

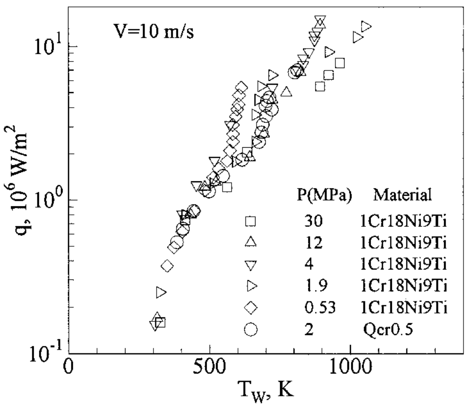

Fig. 2 Effect of pressure on kerosene heat transfer.

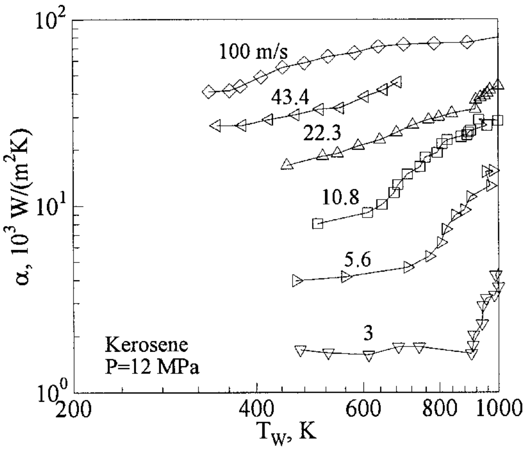

Fig. 3 Effect of velocity on kerosene heat transfer.

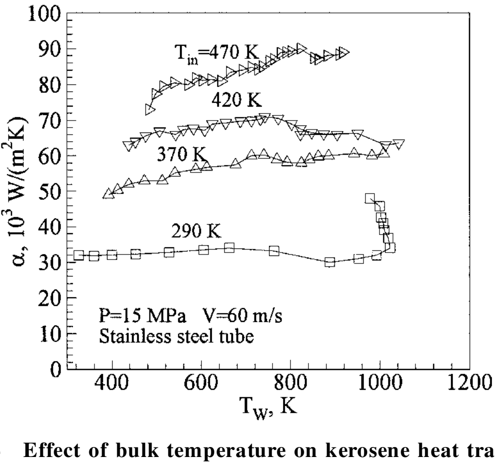

Fig. 4 Effect of bulk temperature on kerosene heat transfer.

The effect of inlet temperature was shown in the tests at a pressure of 15 MPa, velocity of 60 m/s, and various inlet bulk temperatures. The higher the inlet temperatures, the higher heat transfer coefficients (shown in Fig. 4). This results from lower viscosity and higher Reynolds number at higher bulk temperatures.

Tests comparing the performance of rocket kerosene in 2.2 × 0.25-mm stainless-steel (1Cr18Ni9Ti) and copper (QCr0.5) tubes indicate that heat transfer coefficients are not related to test-tube materials (shown in Fig. 2). The preceding observations are applicable to all of the tested types of kerosene, including no. 21 high-density kerosene, aerokerosene, and rocket kerosene.

Figure 5 shows that the forced convection heat transfer test data on kerosene prior to the occurrence of skin boiling or pseudoboiling and deposit formation can be correlated using the following equations:

$$Nu = 0.005Re^{0.95}Pr^{0.4}, \quad \text{at} \quad Re < 2 \times 10^4$$

$$Nu = 0.023Re^{0.8}Pr^{0.4}, \quad \text{at} \quad Re > 2 \times 10^4$$

where properties are evaluated at the bulk temperature.

There was no coking in copper tubes because the tubes had burnout before coking occurred, but significant coking occurred in the stainless-steel tubes. Long duration coking tests were performed with heat flux, velocity, and pressure conditions constant, and with heat flux varied and velocity and pressure conditions held constant. The test results indicate the following:

1) At a pressure of 15 MPa and velocity of 20 m/s, coking of rocket kerosene was first detected at a wall temperature of about 650 K.

2) Rates of increase in wall temperature (0.1–2.4 K/min, shown in Fig. 6) caused by rocket kerosene coking were lower than those of aerokerosene (2–5.1 K/min), because rocket kerosene was refined. The coking thermal resistance of rocket kerosene ranged from 0.5 × 10^{-5} to 4.1 × 10^{-5} K m^2/W (shown in Fig. 7).

3) Deposition rates were high in the first 10 min during the coking tests, then the rates decreased and tended to be steady (shown in Figs. 6 and 7). Deposition sometimes decreased after coking.

4) Deposition in nitrogen-pressurized tests was less than that in air-pressurized tests. As shown in Fig. 8, in tests with air pressurization, coking temperature was lower and coking thermal resistance was higher because the oxygen in air increases deposition.

5) The quantity of suspended materials in kerosene could be reduced by filtering through a deerskin filter, and so deposition decreased after filtration.

Deposition from fuels at high temperatures is the agglutination of carbonaceous solid pellets cohered by colloid material.[15] Deposition mainly results from the agglomeration of oxidative nonhydrocarbon chemicals in the fuels. The sulfur, nitrogen, and oxygen contents of the deposits are always higher than those of the original fuels. The thermal stability of the fuels will improve and fuel deposit formation will decrease significantly if nonhydrocarbon materials are eliminated from the fuels or if the fuels are pressurized with inert gas, nitrogen, or fuel vapor. As proved by the preceding tests, the coking of

Table 3 Thermal properties of hydrocarbon fuels

Fuel	T_s, K	P_{cr}, MPa	T_{cr}, K	ρ, 293 K (kg/m^3)	*Cp*, 293 K (kJ/kg K)	*k*, 293 K (W/m K)	μ, 293 K (10^{-3} Pa s)
Methane	112	4.64	191	422 (113 K)	3.426 (112 K)	0.195 (112 K)	0.098 (112 K)
Propane	231	4.26	370	584 (230 K)	2.24 (233 K)	0.123 (233 K)	0.205 (233 K)
Aerokerosene	——	2.39	598	781.7	2.08	0.148	1.141
No. 21 kerosene	——	——	——	895.1	1.64	——	2.363
Rocket kerosene	——	2.50	677	833	2.0	0.1385	1.96
RP-1	——	2.2	668	810	1.9	0.104	1.93

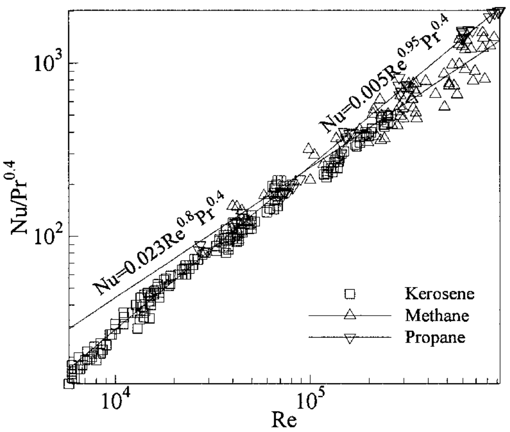

Fig. 5 Forced convection heat transfer correlation of hydrocarbon fuels.

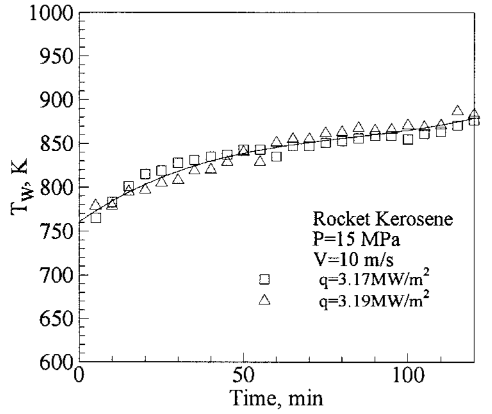

Fig. 6 Temperature variation in rocket kerosene coking tests.

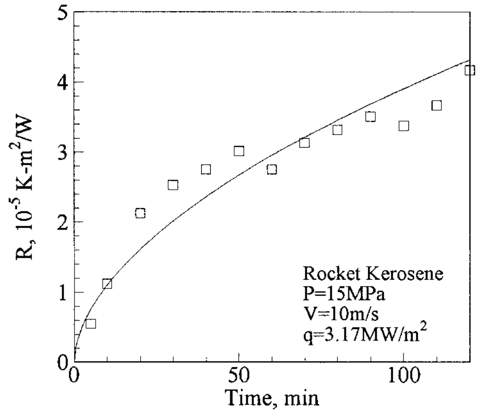

Fig. 7 Coking thermal resistance in rocket kerosene coking tests.

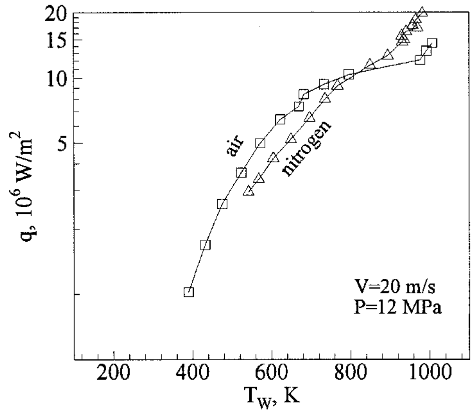

Fig. 8 Effect of gas pressurization on heat transfer.

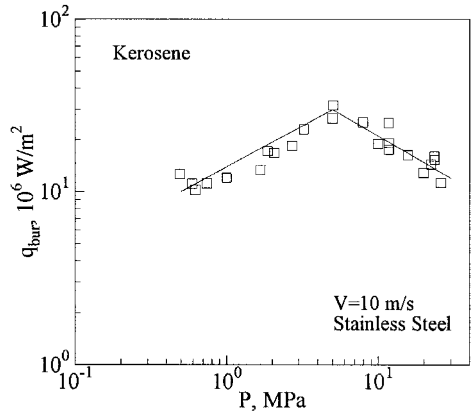

Fig. 9 Effect of pressure on burnout heat flux of kerosene.

kerosene can be reduced significantly by means of refinement (rocket kerosene), nitrogen pressurization, and filtration.

The heat fluxes at which test tubes burn out were also investigated. The burnout heat flux for test tubes is closely related to medium cooling performances, test conditions, tube structure, tube material, and tube strength at high temperatures. The heat flux at which a test tube burns out is different from the critical heat flux. Both are valuable in engine design.[16]

At a velocity of 10 m/s, the effect of pressure on burnout heat flux is shown in Fig. 9. It can be seen that burnout heat flux ($q_{\rm bur}$) increases with increasing pressure, and peaks at about 5 MPa, then decreases. Figure 10 shows the effect of velocity on burnout heat flux at 12 MPa. The burnout heat flux increases with increasing velocity. At a pressure of 25 MPa, the copper test tubes burned out at coolant-side wall temperatures of about 670 K and the stainless-steel test tubes burned out at about 1070 K.

Under all of the test temperature conditions, all kinds of kerosene were compatible with stainless steel, and rocket kerosene was compatible with copper. That is, the fuel did not attack the tube material.

Based on the previous discussion, the following observations can be made: the heat transfer coefficients of kerosene are low prior to skin boiling or pseudoboiling; boiling or pseudoboiling does occur for kerosene, however, and raises the heat transfer coefficients at high wall temperatures; coking was detected at wall temperatures above 650 K for rocket kerosene, with the coking temperature increase rates ranging from 0.1 to 2.4 K/min and thermal resistance from 0.5×10^{-5} to 4.1×10^{-5} K m^2/W.

Methane Test

The test conditions for methane are shown in Table 1. As shown in Fig. 11, heat transfer coefficients of methane were rather high at wall temperatures below about 320 K. The heat transfer coefficients, for instance, were 55–60 kW/m^2 K at a pressure of 12 MPa and velocity of 30 m/s. The high heat transfer coefficients of methane result from its high thermal conductivity and specific heat and low viscosity, as shown in Table 3.

No significant boiling or pseudoboiling phenomenon was detected under our test conditions for methane (shown in Fig. 11). A significant decrease in the methane heat transfer coefficients occurred at wall temperatures around 320 K. At a velocity of 30 m/s, for example, the heat transfer coefficient decreased to 2×10^4 W/m^2 K at a wall temperature of 800 K. The mechanism of the change of methane heat transfer coefficients is not yet clearly understood. The critical temperature of methane is rather low, and so near-wall fluid can easily reach the critical temperature and may cause the near-wall phase transition. In this case, methane thermal properties would change sharply.[16] This may be the most likely reason for the change in methane heat transfer coefficients.

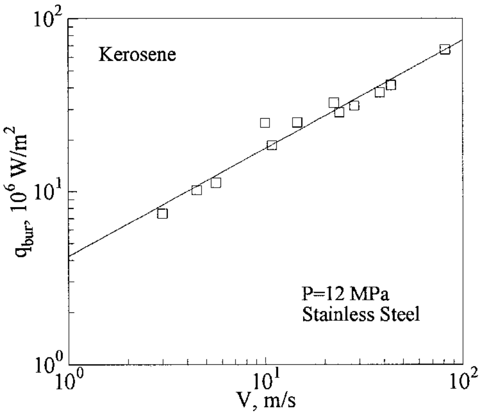

Fig. 10 Effect of velocity on burnout heat flux of kerosene.

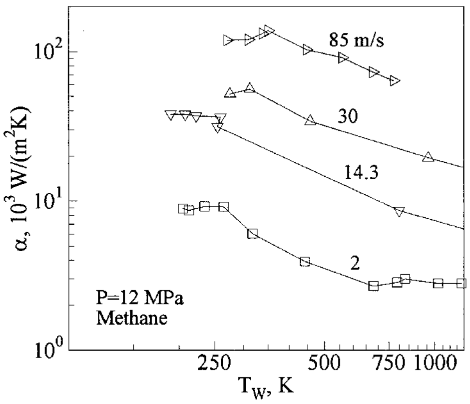

Fig. 11 Heat transfer coefficients of methane.

For methane, test data for conditions prior to the decrease in heat transfer coefficients can be correlated with the equation, $Nu = 0.023Re^{0.8}Pr^{0.4}$, at $Re = 3.5 \times 10^4\text{–}3 \times 10^6$, where properties are evaluated at the bulk temperature, as shown in Fig. 5.

No coking was detected in any of the methane tests; the inner surfaces of the tubes were clean.

The burnout heat flux for methane increased with increasing pressure and velocity (shown in Figs. 12 and 13). Burnout heat fluxes for methane were lower than those for kerosene because of the low heat transfer coefficients of methane at high wall temperatures.

Methane was compatible with stainless steel and copper.

Propane Tests

The test conditions for propane are shown in Table 1. The tests were conducted with 95% pure propane.

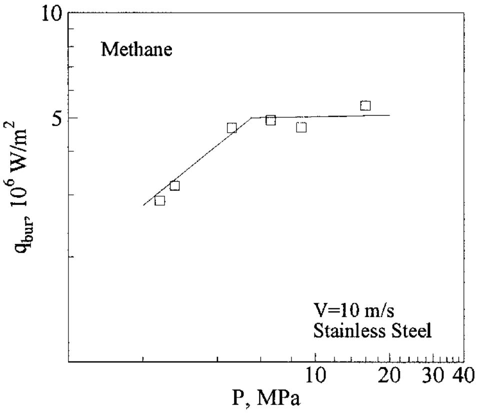

Fig. 12 Effect of pressure on burnout heat flux of methane.

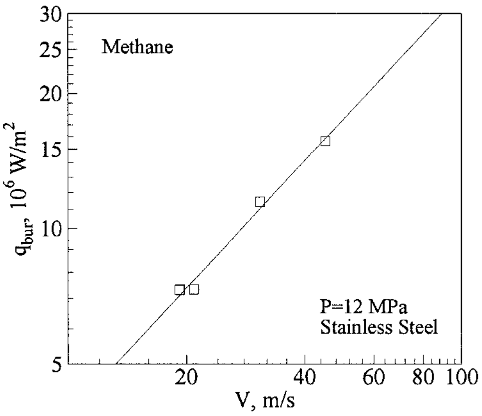

Fig. 13 Effect of velocity on burnout heat flux of methane.

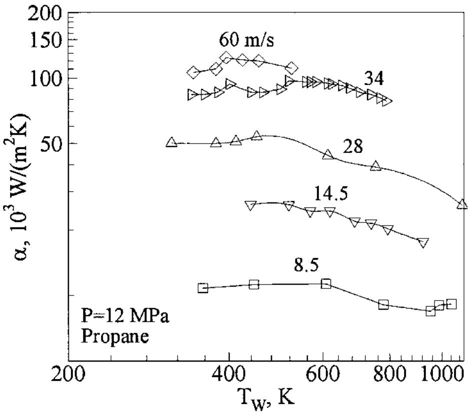

Fig. 14 Heat transfer coefficients of propane.

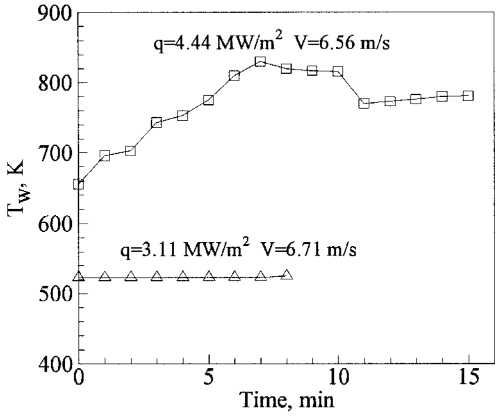

Fig. 15 Temperature variation in propane coking tests.

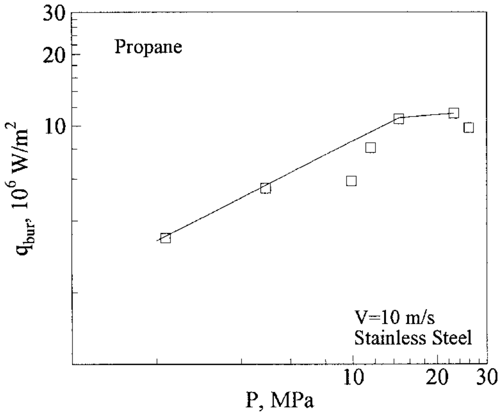

Fig. 16 Effect of pressure on burnout heat flux of propane.

As shown in Fig. 14, heat transfer coefficients for propane also decreased, as in the methane tests. However, the wall temperatures at which heat transfer coefficients of propane began to decrease were higher than those for methane, and the decrease was not so significant as in the case of methane.

For propane, the test data before the decrease in the heat transfer coefficients are correlated using the equation, $Nu = 0.005Re^{0.95}Pr^{0.4}$, at $Re = 2 \times 10^4$–9×10^5, where properties are evaluated at the bulk temperature, as shown in Fig. 5.

In the propane tests presented in Table 1, the inner surfaces of the test tubes became slightly black. In later special coking tests,[10] coking occurred for propane in stainless-steel tubes at wall temperatures between 650 and 670 K. The increase in wall temperature because of propane coking is shown in Fig. 15.

The burnout heat flux of propane increased with increases in pressure and velocity (shown in Figs. 16 and 17).

Propane was compatible with stainless steel.

Cooling Characteristics of Hydrocarbon Fuels

As shown in Fig.18, the heat transfer performances of methane and propane are much better than that of kerosene at low wall temperatures. Significant skin boiling or pseudoboiling does not occur in methane and propane tests but does occur for kerosene. When the wall temperatures are a certain amount higher than the critical temperatures of methane and propane, the heat transfer coefficients decrease at different rates. Thus, kerosene heat transfer coefficients are higher than those of methane and propane at high wall temperatures. The final results of the preceding changes can be shown from the burnout heat fluxes (shown in Figs. 9, 10, 12, 13, 16, and 17).

No coking was detected for methane in stainless-steel and copper tubes. Coking was present for propane in stainless-steel and copper tubes and was more severe than for kerosene under the same conditions.

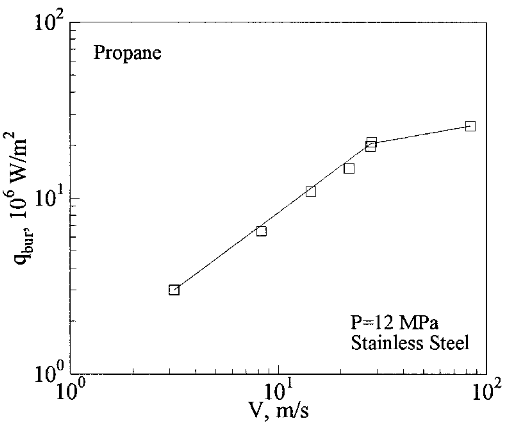

Fig. 17 Effect of velocity on burnout heat flux of propane.

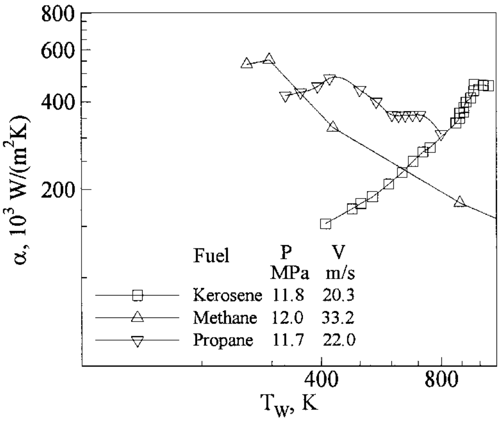

Fig. 18 Heat transfer coefficients of hydrocarbon fuels.

When using hydrocarbon fuels as coolants, close attention should be paid to the cooling characteristics of hydrocarbon fuels. Readers can refer to the test results presented in this paper to select suitable coolants for their own cooling design needs.

Conclusions

1) The forced convection heat transfer correlations of single-phase methane, propane, and kerosene are methane: $Nu = 0.023Re^{0.8}Pr^{0.4}$, at $Re = 3.5 \times 10^4$–3×10^6; propane: $Nu = 0.005Re^{0.95}Pr^{0.4}$, at $Re = 2 \times 10^4$–9×10^5; and kerosene: $Nu = 0.005Re^{0.95}Pr^{0.4}$, at $Re < 2 \times 10^4$, and $Nu = 0.023Re^{0.8}Pr^{0.4}$, at $Re > 2 \times 10^4$.

2) Heat transfer performances of methane and propane are superior than that of kerosene at low wall temperatures. Heat transfer coefficients of methane and propane decrease at wall temperatures a certain amount above their respective critical temperatures and the coefficients of kerosene increase at similar wall temperatures.

3) No coking was detected in methane tests. Coking was present for propane in stainless-steel tubes.

4) Coking of rocket kerosene was detected at wall temperatures around 650 K. During rocket kerosene coking, the range of rising rates of wall temperature is from 0.1 to 2.4 K/min and coking thermal resistance ranges from 0.5×10^{-5} to 4.1×10^{-5} K m²/W.

Acknowledgment

Presented as Paper 3.8 at the 3rd International Symposium on Space Propulsion, Beijing, People's Republic of China, August 11–13, 1997.

References

[1] Masters, P. A., and Aukerman, C. A., "Deposit Formation in Hydrocarbon Rocket Fuels with an Evaluation of a Propane Heat Transfer Correlation," NASA TM-82911, June 1982.

[2] Cook, R. T, "Advanced Cooling Techniques for High Pressure Hydrocarbon-Fueled Rocket Engines," AIAA Paper 80-1266, June 1980.

[3] Michel, R. W., "Combustion Performance and Heat Transfer Characterization of LOx/Hydrocarbon Type Propellants," NASA-CR-171712, Sept. 1983.

[4] Michel, R. W., "Combustion Performance and Heat Transfer Characterization of LOx/Hydrocarbon Type Propellants," NASA-CR-171713, April 1983.

[5] Giovanetti, A. J., Spadaccini, L. J., and Szetela, E. J., "Deposit Formation and Transfer in Hydrocarbon Rocket Fuels," NASA-CR-168277, Oct. 1983.

[6] Giovanetti, A. J., Spadaccini, L. J., and Szetela, E. J., "Deposit Formation and Transfer in Hydrocarbon Rocket Fuels," AIAA Paper 84-0512, Jan. 1984.

[7] Kirby, F. M., "Methane Heat Transfer Investigation," NASA-CR-171199, Nov. 1984.

[8] Liang, K. M., "Heat Transfer Test Investigation on Hydrocarbon Rocket Fuels (Kerosene)," *Journal of Propulsion Technology*, No. 1, 1988, pp. 65, 66.

[9] Zhang, Z. G., and Zheng, X. Q., "Experimental Investigation on LOx/Propane Thrust Chamber," *Journal of Propulsion Technology*, No. 1, 1992, pp. 50–56.

[10] Zhou, X. D., Zhang, B. J., and Zhong, S., "The Experimental Investigation on the Coking Characteristic of Propane by Heated Tube Test," *Journal of Propulsion Technology*, No. 5, 1991, pp. 27–33.

[11] Mehta, G., Stone, W., Ingram, C., Bai, S. D., and Sanders, T., "Comparative Testing of Russian Kerosene and RP-1," AIAA Paper 95-2962, July 1995.

[12] Thongchun, Z. C., "Regenerative Cooling of High Pressure Hydrocarbon Rocket Combustors," *Journal of the Japan Society for Aeronautical and Space Sciences*, Vol. 37, No. 427, 1989, pp. 28–34.

[13] Rosenberg, S. D., and Gage, M. L., "Compatibility of Hydrocarbon Fuels with Booster Engine Combustion Chamber Liners," AIAA Paper 88-3215, July 1988.

[14] Rosenberg, S., and Gage, M., "Corrosion Prevention in Hydrocarbon-Fueled Booster Engine Combustion Chamber Liners," AIAA Paper 89-2738, July 1989.

[15] Baloke, K. K., *Aeronautical Fuels and Rocket Fuels*, Translated by Zhang, F., China Press of Industry, Beijing, PRC, 1965.

[16] Chen, G. Y., "Heat Transfer," *Theory of Liquid Rocket Engines*, edited by G. Q. Liu, China Press of Aerospace, Beijing, PRC, 1993, pp. 320–325.